# EVALUATION OF HYDRODYNAMIC BEARINGS WITH GEOMETRIC DESCONTINUITIES

**Tiago Henrique Machado, tiagomh@fem.unicamp.br**
**Katia Lucchesi Cavalca, katia@fem.unicamp.br**
Laboratory of Rotating Machinery – Faculty of Mechanical Engineering – Postal Box 6122
University of Campinas – UNICAMP - 13083-970, Campinas, SP, Brazil

**Abstract.** *Hydrodynamic bearings are widely used in rotating machines, being the element responsible for the interaction between the rotor and the supporting structure. Therefore, in order to describe the dynamic behavior of the rotating shafts, it is necessary to know the journal bearings characteristics. The proposed methodology for the design and development of these components, optimizing their performance and, therefore, involving research and understanding of the phenomena associated with hydrodynamic lubrication, as well as the design parameters, directly meets this demand. For this reason, the purpose of this paper is to analyze the static and operational characteristics of different configurations of radial hydrodynamic bearings. The objective of this project is to develop and implement a consistent mathematical representation for the static model of the hydrodynamic bearing through the Reynolds equation and thereby obtaining the pressure distribution in the bearing, to evaluate the performance of different geometries in severe conditions, high speeds and high-applied load. A numerical model for the solution of Reynolds equation, with help from the Bernoulli equation, obtains the pressure field generated inside the oil film. The numerical approach used in this study is done using the finite volume method. The choice of this method was made due to their widespread use in the numerical simulation of phenomena of fluid dynamics and heat transfer. The paper presents an analysis for three different geometries of bearings, a cylindrical, an elliptical and a three-lobe. In addition to the different geometries, the paper also proposes a study on the effect of some geometric discontinuities in the behavior of the bearings. The discontinuities were introduced in the form of axial grooves, and its effect is then compared with the performance of bearings without these grooves. The grooves bring new elements to the behavior of the bearing, such as reducing pressure on the oil film and greater retention of fluid between the shaft and bearing.*

***Keywords****: Hydrodynamic Lubrication; Finite Volume Method; Multi-Lobe Bearings; Grooves Effects.*

## 1. INTRODUCTION

The study of rotating machinery occupies a prominent position in the context of machines and structures in view of the significant number of typical phenomena in the operation of such equipment. The existence of a rotating component supported by bearings and transmitting power creates a family of problems that are found in several machines such as compressors, turbines, pumps, engines, among others. Such equipment is often an integral part of production plants or power generation plants, in which a sudden stop can cause great financial losses. Therefore, there is an evident need of understanding the phenomena related to rotating machinery, more significantly, in relation to components involved in the interface between fixed and moving components, such as bearings.

The interest in understanding the phenomena associated with hydrodynamic lubrication is not recent in the academic field. The first studies related to this subject are dated from early 1880. At that time, three different papers, with few years of each other, and independently developed, understood and began to explain the mechanism of hydrodynamic lubrication: N. P. Petrov (1836-1920), B. Tower (1845-1904) and O. Reynolds (1842-1912). These authors have in common the perception that the lubrication process did not occur due to mechanical interaction between two solid surfaces, but because of the characteristics of the fluid film separating them. This is the fundamental aspect of hydrodynamic lubrication and from this new knowledge in a short period of time; the theoretical and experimental foundations began to be established. Among these authors, Reynolds deserves noteworthy. He established the differential equation that defines the pressure field between two surfaces with relative motion.

During the 20th century, several scientists attempted to solve the Reynolds equation by means of analytical and numerical methods. In 1904, Sommerfeld published an analytical solution for the Reynolds equation, applied to long bearings. This solution was obtained by integrating the Reynolds equation from new boundary conditions, considering the absence of oil leakage at the ends of the bearing. Ocvirk proposed in 1952, a solution of Reynolds equation applied to short bearings. This solution neglects the term that takes into account the circumferential flow of the bearing, considering that it is small when compared to the flow in the axial direction of the shaft.

The first use of computers for the solution of Reynolds equation, with the correct boundary conditions, was made in 1956 by Pinkus. Pinkus examined the pressure distribution in elliptical bearings (1956), partial arcs bearings (1958) and three-lobe bearings (1959), experimentally investigating the instability of these geometries.

With very little time, a large spectrum of solutions had been developed for numerous types of bearings, both the gas and those who use oil as a lubricant. The most important contribution of information technology, in this field, was the fact that within five years, the solution for finite bearings had been established and that time is extremely short compared to the time of the beginning of Tribology.

The researches involving the numerical solution of the pressure distribution in hydrodynamic bearings have been limited, in most cases, to use the methods of finite differences or finite elements. Objectively, there are no advantages or disadvantages in choosing one method or another; all of them serve the purpose of finding the solution of the conservative equation in a discretized domain. However, the differences become evident when considering the characteristics connected with the conditions of use and application. Works such as those conducted by Singhal (1981) and Colin (1971) show the applicability of the method of finite differences in fluid dynamics and lubrication problems, especially for the possibility of a discretization of Reynolds equation by nodal points. Similarly is the finite element approach, but in this case the application is more complex in the mathematical point of view.

The use of the finite volume method is less common for tribology researchers, probably due to the poor diffusion of the technique among solid mechanics scholars. One of the main references about the method was published by Patankar (1980), with simple and direct approaches, bringing the main concepts of the method, and even focusing on the use of the method in problems of heat transfer, Patankar dedicates some chapters to problems of fluid mechanics and its main nonlinear characteristics. Still in the line of conceptual finite volume method, another reference is the work of Maliska (2004), with extensive computational approach and the issues surrounding the development of programs for CFD (Computational Fluid Dynamic), or the computational study of the fluid dynamics, it meets almost all the basics aspects for those who want to develop their first models using the method.

Some of the most relevant papers with FVM (Finite Volume Method) applied to journal bearings were conducted by Castelli (1968), who did a review on numerical methods for bearings and proposed some solutions and studies. More recently, Arghir et al. (2001) worked with the solution for triangle-based volumes to the problem of oil film bearings. Later, in another paper, Arghir et al (2002) proposed a solution to problems of discontinuity in the oil film applied to cylindrical bearings. The latest paper clearly showed the characteristics of the assembly and placement of the meshes in situations where there are discontinuities in the oil film, caused by grooves inside the bearings. References on a mesh for flow analysis at the boundaries of the domain were shown in a study conducted by Kogure et al. (1983). In the case of the coordinate system transformation to an adaptive mesh, Kang et al. (1996) may be cited for their contribution to the approach of the discontinuities in the oil film.

## 2. THEORY AND RESULTS

### 2.1 Reynolds Equation

The basis of the modern theory of hydrodynamic lubrication is the Reynolds equation. Its solution gives the pressure distribution in the lubricating fluid. The pressure field is the information needed for the solution of most problems in the analysis of hydrodynamic bearings, and hydrodynamic reaction forces are derived from the integration of this pressure field.

The Reynolds equation for lubrication is evaluated in the specific case where the thickness of the oil film is discontinuous. This procedure was accomplished by Arghir et al. (2002). In their paper it was presented a description of the approach in one dimension and results for a thrust bearing in one and two dimensions. The present work describes this procedure for different journal bearings in two dimensions. For this approach, considering the balance of flows of lubricating fluid in each control volume, the Reynolds equation must be written in terms of these flows. The flow of lubricating fluid in a bearing occurs due to the shearing of the fluid, caused by the relative motion of the shaft regarding to the bearing, dragging the lubricating oil; and due to pressure gradients.

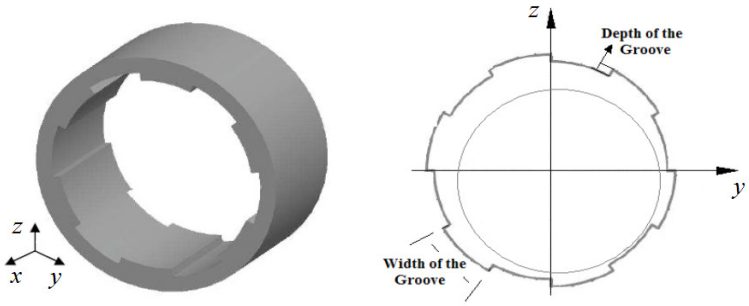


Figure 1: Bearings with Discontinuities and the Representation of the Coordinate System

Considering the $y$ and $x$ coordinate system, the flows of fluid per unit of length in each of the two directions are given by:

$$q_y = \frac{U}{2}h - \frac{h^3}{12\mu}\frac{\partial p}{\partial y} \tag{1}$$

$$q_x = -\frac{h^3}{12\mu}\frac{\partial p}{\partial x} \tag{2}$$

With the expressions for the flow in each direction, the continuity equation for the fluid present in the bearing clearance can be written as follows:

$$\frac{\partial q_y}{\partial y} + \frac{\partial q_x}{\partial x} = \frac{\partial h}{\partial t} \tag{3}$$

Bringing equations (1) and (2) into equation (3), the Reynolds' equation is obtained.

$$\frac{\partial}{\partial y}\left(h^3\frac{\partial p}{\partial y}\right) + \frac{\partial}{\partial x}\left(h^3\frac{\partial p}{\partial x}\right) = 6\mu U\frac{\partial h}{\partial y} + 12\mu\frac{\partial h}{\partial t} \tag{4}$$

where $p$ is the pressure generated within the fluid, $t$ is time, $y$ and $x$ are the cartesian coordinates in the inertial reference system, as shown in Fig. 1, μ is the absolute viscosity of the lubricant, U is the peripherical velocity of the rotor and h is the film thickness, according to the bearing geometry.

In this paper the bearing is analyzed statically (even with the rotation of the shaft, the term "static analysis" is used by researchers (see Lund 1987)), thus, the term $\frac{\partial h}{\partial t}$ present in equations 3 and 4 is neglected.

### 2.2 Calculation of the Pressure Distribution with Film Discontinuities through the Finite Volume Method

According Arghir et al. (2002), in the immediate vicinity of a film thickness discontinuity, the pressure has very rapid and almost abrupt variation. This is due to an embedded recirculation zone which cannot be described by lubrication theory, which can only handle flows with almost parallel streamlines. According to the simplifying assumptions of lubrication, this rapid variation must be located at the discontinuity and the pressure field should be discontinuous. The usual practice to describe the rapid pressure variation in the theoretical lubrication model is to write the generalized Bernoulli equation immediately before and after the discontinuity.

$$P^- + \frac{\rho U^{-2}}{2} = P^+ + \frac{\rho U^{+2}}{2} + \xi\frac{\rho\left[MAX\left(U^-, U^+\right)\right]^2}{2} \tag{5}$$

The pressure drop coefficient $\xi$ takes into account an additional energy loss due to viscous effects and it is an addition contribution to the analysis. This additional equation should somehow be linked to the solution of the Reynolds equation in the oil film.

For the numerical solution, we start from equation 3, considering static analysis $\left(\frac{\partial h}{\partial t} = 0\right)$, rearranging as follows:

$$\partial q_y \partial x + \partial q_x \partial y = 0 \tag{6}$$

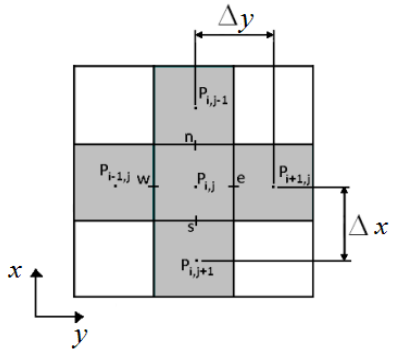


Figure 2: Mesh of a Finite Volume Enhancing the Point i, j

For a volume (i, j), shown in Fig. 2, the following expression is obtained:

$$\left(q_{i,j}^{e}-q_{i,j}^{w}\right)\Delta x+\left(q_{i,j}^{n}-q_{i,j}^{s}\right)\Delta y=0 \tag{7}$$

In which:

$$q_{i,j}^{e}=\left[-\left(\frac{h^3}{12\mu}\right)_{i,j}^{e}\frac{P_{i,j}^{e}-P_{i,j}}{y_{i+1/2,j}-y_{i,j}}+\frac{U\,h_{i,j}^{e}}{2}\right] \qquad q_{i,j}^{w}=\left[-\left(\frac{h^3}{12\mu}\right)_{i,j}^{w}\frac{P_{i,j}-P_{i,j}^{w}}{y_{i,j}-y_{i-1/2,j}}+\frac{U\,h_{i,j}^{w}}{2}\right]$$

$$q_{i,j}^{n}=\left[-\left(\frac{h^3}{12\mu}\right)_{i,j}^{n}\frac{P_{i,j}^{n}-P_{i,j}}{x_{i,j+1/2}-x_{i,j}}\right] \qquad q_{i,j}^{s}=\left[-\left(\frac{h^3}{12\mu}\right)_{i,j}^{s}\frac{P_{i,j}-P_{i,j}^{s}}{x_{i,j}-x_{i,j-1/2}}\right] \tag{8}$$

For flow continuity, the equilibrium is needed, in each control volume, as follow:

$$q_{i-1,j}^{e}=q_{i,j}^{w} \tag{9}$$

$$q_{i,j}^{e}=q_{i+1,j}^{w} \tag{10}$$

$$q_{i,j-1}^{n}=q_{i,j}^{s} \tag{11}$$

$$q_{i,j}^{n}=q_{i,j+1}^{s} \tag{12}$$

Substituting relations (8) in (9), the following expression is obtained:

$$\left[-\left(\frac{h^3}{12\mu}\right)_{i-1,j}^{e}\frac{P_{i-1,j}^{e}-P_{i-1,j}}{y_{i-1/2,j}-y_{i-1,j}}+\frac{U\,h_{i-1,j}^{e}}{2}\right]=\left[-\left(\frac{h^3}{12\mu}\right)_{i,j}^{w}\frac{P_{i,j}-P_{i,j}^{w}}{y_{i,j}-y_{i-1/2,j}}+\frac{U\,h_{i,j}^{w}}{2}\right] \tag{13}$$

To simplify the equation, two new variables are introduced:

$$b_{i-1,j}^{e}=\left[\frac{-\left(\frac{h^3}{12\mu}\right)_{i-1,j}^{e}}{y_{i-1/2,j}-y_{i-1,j}}\right]=\left[\frac{-\left(\frac{h^3}{12\mu}\right)_{i-1,j}^{e}}{\Delta y/2}\right] \qquad b_{i,j}^{w}=\left[\frac{-\left(\frac{h^3}{12\mu}\right)_{i,j}^{w}}{y_{i,j}-y_{i-1/2,j}}\right]=\left[\frac{-\left(\frac{h^3}{12\mu}\right)_{i,j}^{w}}{\Delta y/2}\right] \tag{14}$$

Substituting (14) in (13), the following expression is obtained:

$$b_{i-1,j}^{e}P_{i-1,j}^{e}-b_{i-1,j}^{e}P_{i-1,j}=b_{i,j}^{w}P_{i,j}-b_{i,j}^{w}P_{i,j}^{w}+\frac{U}{2}(h_{i,j}^{w}-h_{i-1,j}^{e}) \tag{15}$$

As previously mentioned, the pressure field at the interface of discontinuities should be discontinuous, and to describe the rapid variation on the pressure, in the theoretical model of lubrication, it is necessary to write the generalized Bernoulli equation (5) immediately before and after the discontinuity, i.e., in positions north, south, east and west of each control volume.

Thus, to the west side of the control volume, the Bernoulli equation can be written as:

$$P_{i-1,j}^{e}+\frac{\rho(V_{i-1,j}^{e})^2}{2}=P_{i,j}^{w}+\frac{\rho(V_{i,j}^{w})^2}{2}+\xi\frac{\rho\left[\max(V_{i-1,j}^{e},V_{i,j}^{w})\right]^2}{2} \tag{16}$$

In which the velocities are given by:

$$V_{i-1,j}^{e}=\frac{q_{i-1,j}^{e}}{h_{i-1,j}^{e}} \qquad V_{i,j}^{w}=\frac{q_{i,j}^{w}}{h_{i,j}^{w}} \tag{17}$$

The $\xi$ coefficient takes into account an additional energy loss due to viscous effects. In this analysis, for the sake of simplicity, this coefficient is considered null, i.e. $\xi = 0$, making equation (16) as follows:

$$P^{e}_{i-1,j} = P^{w}_{i,j} + A_{i-1/2,j} \tag{18}$$

In which:

$$A_{i-1/2,j} = \frac{\rho(V^{w}_{i,j})^2}{2} - \frac{\rho(V^{e}_{i-1,j})^2}{2} \tag{19}$$

Substituting $P^{e}_{i-1,j}$ from equation (18) in equation (15) and isolating $P^{w}_{i,j}$, the following expression is obtained:

$$P^{w}_{i,j} = \frac{b^{e}_{i-1,j}P_{i-1,j} + b^{w}_{i,j}P_{i,j} - b^{e}_{i-1,j}A_{i-1/2,j} + \left[\frac{U}{2}(h^{w}_{i,j} - h^{e}_{i-1,j})\right]}{\left(b^{e}_{i-1,j} + b^{w}_{i,j}\right)} \tag{20}$$

The procedure to obtain the pressure on the remaining edges, $P^{e}_{i,j}$, $P^{s}_{i,j}$ e $P^{n}_{i,j}$, is identical to the previously used to find $P^{w}_{i,j}$. Start from equations (10), (11) and (12), it is obtained the following set of equations:

$$P^{e}_{i,j} = \frac{b^{e}_{i,j}P_{i,j} + b^{w}_{i+1,j}P_{i+1,j} + b^{w}_{i+1,j}A_{i+1/2,j} + \left[\frac{U}{2}(h^{w}_{i+1,j} - h^{e}_{i,j})\right]}{\left(b^{e}_{i,j} + b^{w}_{i+1,j}\right)} \tag{21}$$

$$P^{s}_{i,j} = \frac{b^{s}_{i,j}P_{i,j} + b^{n}_{i,j-1}P_{i,j-1} - b^{n}_{i,j-1}A_{i,j-1/2}}{\left(b^{s}_{i,j} + b^{n}_{i,j-1}\right)} \tag{22}$$

$$P^{n}_{i,j} = \frac{b^{n}_{i,j}P_{i,j} + b^{s}_{i,j+1}P_{i,j+1} + b^{s}_{i,j+1}A_{i,j+1/2}}{\left(b^{n}_{i,j} + b^{s}_{i,j+1}\right)} \tag{23}$$

Having found the expressions for the pressure in each of the edges of the control volume, the next step is to find an expression for the pressure at the center of each volume, $P_{i,j}$. Starting from equation (7), substituting the values of equation (8):

$$\left[\left(b^{e}_{i,j}\left(P^{e}_{i,j} - P_{i,j}\right) + \frac{U}{2}h^{e}_{i,j}\right) - \left(b^{w}_{i,j}\left(P_{i,j} - P^{w}_{i,j}\right) + \frac{U}{2}h^{w}_{i,j}\right)\right]\Delta x + \left[b^{n}_{i,j}\left(P^{n}_{i,j} - P_{i,j}\right) - b^{s}_{i,j}\left(P_{i,j} - P^{s}_{i,j}\right)\right]\Delta y = 0 \tag{24}$$

Before taking equations related to the edges of each volume, new variables are introduced to simplify the algebraic manipulations.

$$\begin{aligned} \tilde{T}_{i-1,j} &= \frac{b^{e}_{i-1,j}\,b^{w}_{i,j}}{b^{e}_{i-1,j} + b^{w}_{i,j}} & \tilde{T}_{i+1,j} &= \frac{b^{e}_{i,j}\,b^{w}_{i+1,j}}{b^{e}_{i,j} + b^{w}_{i+1,j}} \\ \tilde{T}_{i,j-1} &= \frac{b^{n}_{i,j-1}\,b^{s}_{i,j}}{b^{n}_{i,j-1} + b^{s}_{i,j}} & \tilde{T}_{i,j+1} &= \frac{b^{n}_{i,j}\,b^{s}_{i,j+1}}{b^{n}_{i,j} + b^{s}_{i,j+1}} \end{aligned} \tag{25}$$

With these new variables, and taking the expressions of each of the edge pressures ($P^{w}_{i,j}, P^{e}_{i,j}, P^{s}_{i,j}$ and $P^{n}_{i,j}$) in equation (24), we derivate an expression for the pressure at the center of each volume:

$$P_{i,j} = \frac{P_{i,j+1}\left(\tilde{T}_{i,j+1}\Delta y\right) + P_{i,j-1}\left(\tilde{T}_{i,j-1}\Delta y\right) + P_{i+1,j}\left(\tilde{T}_{i+1,j}\Delta x\right) + P_{i-1,j}\left(\tilde{T}_{i-1,j}\Delta x\right) + S_{i,j}}{\left(\tilde{T}_{i,j+1} + \tilde{T}_{i,j-1}\right)\Delta y + \left(\tilde{T}_{i+1,j} + \tilde{T}_{i-1,j}\right)\Delta x} \tag{26}$$

In which:

$$S_{i,j} = \frac{U}{2}\left(h^e_{i,j} - h^w_{i,j}\right)\Delta x + \tilde{T}_{i,j+1}A_{i,j+1/2}\Delta y - \tilde{T}_{i,j-1}A_{i,j-1/2}\Delta y + \tilde{T}_{i+1,j}A_{i+1/2,j}\Delta x$$
$$-\tilde{T}_{i-1,j}A_{i-1/2,j}\Delta x + \frac{\tilde{T}_{i+1,j}}{2b^w_{i+1,j}}U\left(h^w_{i+1,j} - h^e_{i,j}\right)\Delta x + \frac{\tilde{T}_{i-1,j}}{2b^e_{i-1,j}}U\left(h^w_{i,j} - h^e_{i-1,j}\right)\Delta x \quad (27)$$

The values $P_{i,j}$ for all points of the discretized mesh are integrated numerically to obtain the radial and tangential resulting hydrodynamic forces on the shaft. These forces are in the local system, and are represented here by $F_r$ and $F_t$:

$$F_r = \sum_{i=1}^{n}\sum_{j=1}^{m} P_{i,j}\cos\theta_i(\Delta y)(\Delta x) \quad (28)$$

$$F_t = \sum_{i=1}^{n}\sum_{j=1}^{m} P_{i,j}\sin\theta_i(\Delta y)(\Delta x) \quad (29)$$

The forces, obtained in the local reference system, are decomposed in the inertial system, using the attitude angle $\phi$. Thus, the following expression is obtained:

$$\begin{Bmatrix} F_y \\ F_z \end{Bmatrix} = \begin{Bmatrix} -F_r\sin\phi + F_t\cos\phi \\ F_r\cos\phi + F_t\sin\phi \end{Bmatrix} \quad (30)$$

For any known geometry and a given eccentricity ratio $\varepsilon$, an equilibrium position of the shaft is determined when $F_y = 0$, which can be obtained by associating the appropriate value of $\phi$.

### 2.3 Results and General Comments

The following sections present the results and analysis of pressure distribution for the three different bearings geometries proposed. Bearings with and without grooves are compared and the influence of these geometric discontinuities is observed.

#### 2.3.1 Pressure Distribution for the Three Different Bearings' Geometry

The first results analyzed are those obtained for the three different bearings' geometries. Analysis are made to a cylindrical bearing, an elliptical bearing and a three-lobe bearing, both preloaded with m=0.4. The geometric characteristics of each type of bearing are shown in Fig. 3.

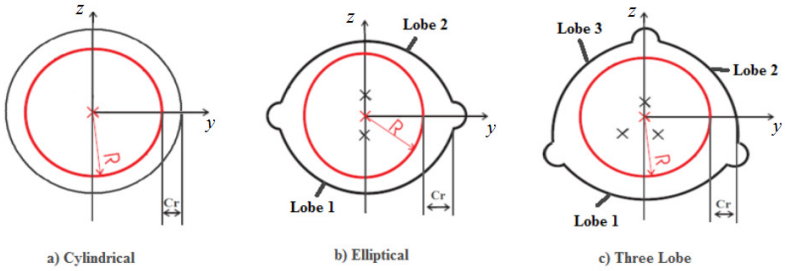


Figure 3: Design of Cylindrical, Elliptical and Three-Lobe Bearings

All these first results are for smooth bearings, without the inclusion of any kind of groove. In all cases, the rotation and applied load are the input parameters. With the value of these variables and the geometric data of the bearing, the equilibrium position is found and the pressure distribution is evaluated. The bearing geometric characteristics and operation parameters are given in Table 1.

Table 1. Bearing input data

| Diameter (m) | Axial Length (m) | Radial Clearance (m) | Load (N) | Viscosity (Pa.s) | Rotation (rpm) |
|---|---|---|---|---|---|
| 0.03 | 0.02 | $9.0 \times 10^{-5}$ | 100 | $5.449 \times 10^{-2}$ | 6800 |

Figures 4 to 9 show the pressure distribution of the first cases examined. In cylindrical and elliptical bearings the origin of circumferential direction is given in the first quadrant. For the three-lobe bearing, as the beginning of any of its lobes coincides with no beginning of a quadrant, the pressure distribution is plotted from the lower lobe of the bearing.

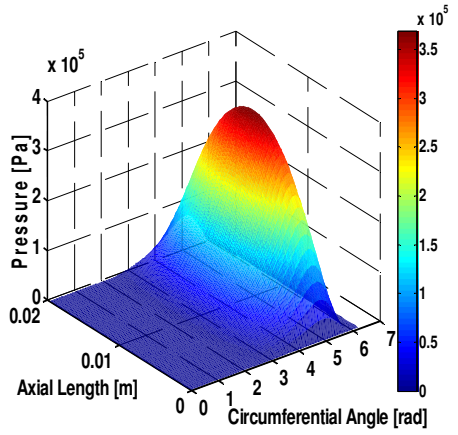


Figure 4: Pressure Distribution Cylindrical Bearing

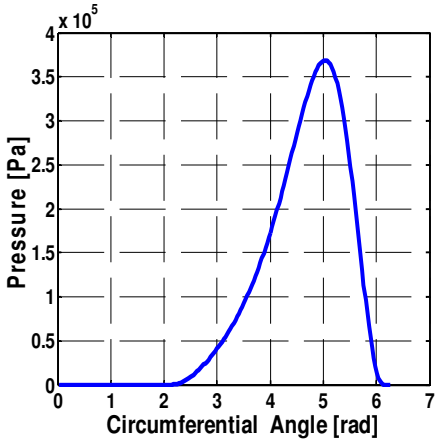


Figure 5: Center Line Pressure Cylindrical Bearing

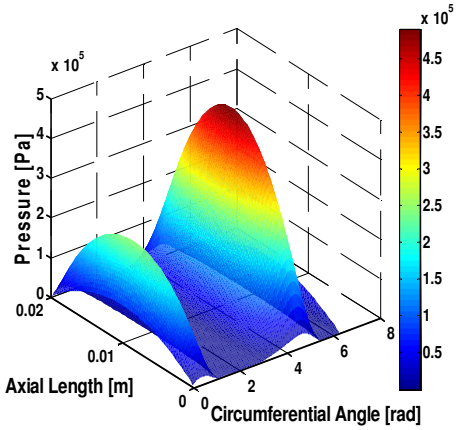


Figure 6: Pressure Distribution Elliptical Bearing

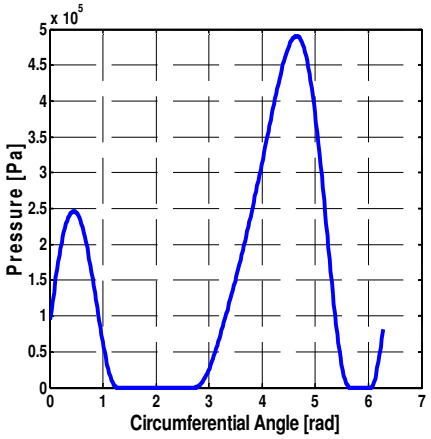


Figure 7: Center Line Pressure Elliptical Bearing

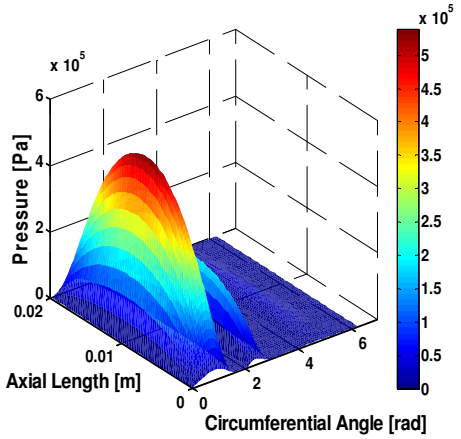


Figure 8: Pressure Distribution Three-Lobe Bearing

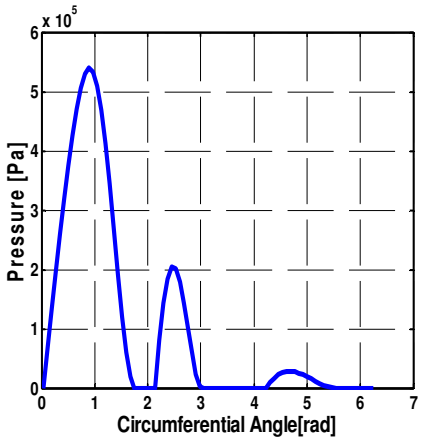


Figure 9: Center Line Pressure Three-Lobe Bearing

Fig. 6 and Fig.7 shows the presence of two peaks of pressure for an elliptical bearing, where 0 to $\pi$ represents the upper lobe of the bearing and $\pi$ to $2\pi$, the lower lobe (Fig. 3b). This can be explained, for this type of bearing, by the fact that for low eccentricity ratios, we have the shaft located on the upper semi-plane of the bearing, making the oil film present in the upper lobe to be compressed, generating larger reaction forces and, consequently, a pressure field in that region.

As the three-lobe bearing is composed by three lobes, it can be notice that its arcs are of 120° (Fig. 3c). The first peak of pressure is related to the lower lobe (1), the central peak corresponds to the right lobe (2) and the last peak, to the left lobe (3). It can be noted by the graphs, Fig. 8 and Fig. 9, the highest pressure is on the lower lobe. The right lobe of the distribution has a slightly higher peak of pressure than the left lobe.

### 2.3.2 Pressure Distribution for the Bearings with Axial Grooves

The influence of axial grooves in the static behavior of the bearings is now evaluated for the case of cylindrical, elliptical and three-lobe bearings. The most important characteristics of these grooves are shown in Fig. 1. For this analysis, the number of the grooves is fixed in 6 and the width of the grooves is fixed at 8mm for all cases analyzed. For all kinds of bearings, the results are shown for the depth of grooves of 0.01mm and 0.1mm. The bearings used have the same input data presented in Table 1. For lobular bearings the preload used in this analysis is m=0.2. As could be noted in the previous figures, only with the analysis of the Center Line Pressure is already possible to notice the influence of the desired parameters. Therefore, for the next cases, only this type of graph will be presented.

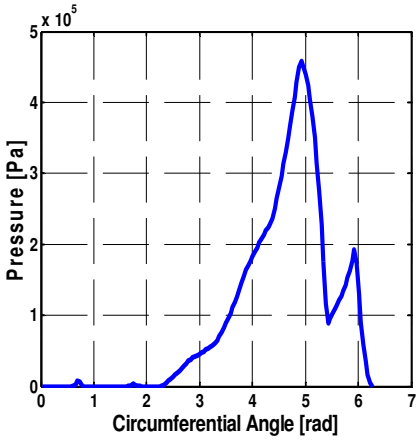


Figure 10: Center Line Pressure Cylindrical Bearing each Groove with 0.01mm of Depth

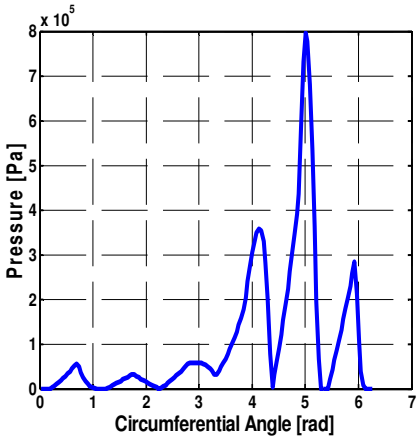


Figure 11: Center Line Pressure Cylindrical Bearing each Groove with 0.1mm of Depth

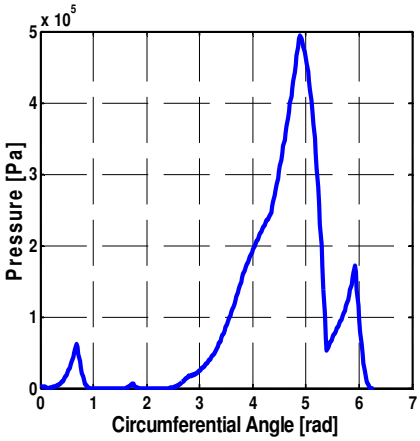


Figure 12: Center Line Pressure Elliptical Bearing each Groove with 0.01mm of Depth

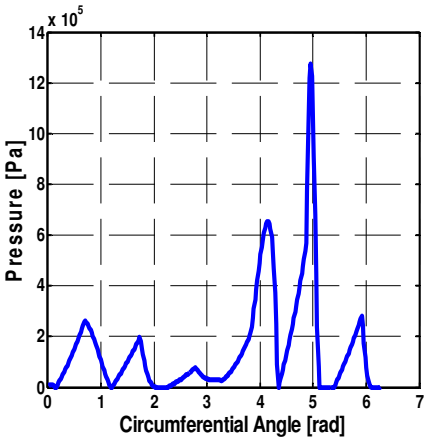


Figure 13: Center Line Pressure Elliptical Bearing each Groove with 0.1mm of Depth

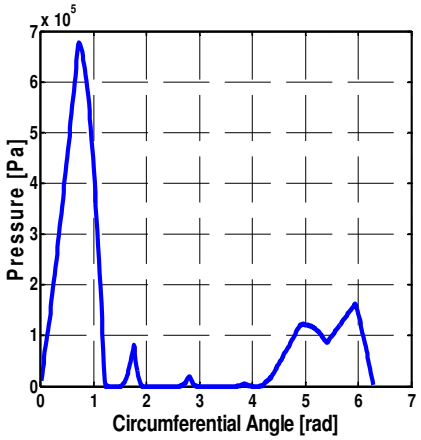


Figure 14: Center Line Pressure Three-Lobe Bearing each Groove with 0.01mm of Depth

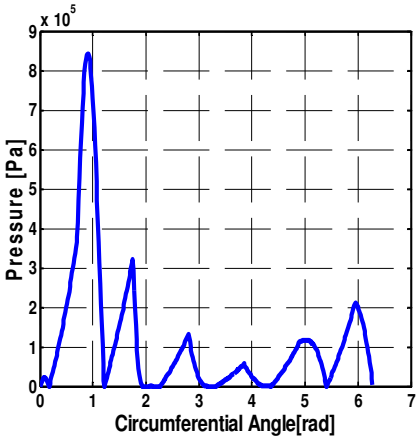


Figure 15: Center Line Pressure Three-Lobe Bearing each Groove with 0.1mm of Depth

In Figs. 10 to 15 the presence of six axial grooves may be noted, being one near the origin, and the others equally spaced around the circumference of the bearings. It can be observed that increasing the depth of the groove, the peak of pressure that appears in the vicinity of that groove also increases. This fact can be explained by the decreasing in the oil film thickness in this region.

The behavior of lobular bearings (elliptical and three-lobe) regarding to the grooves is very similar to that found in cylindrical bearings. First, it can be seen that the presence of the grooves not only makes the rising of new peaks of pressure, but also divided the existing peaks in the smooth bearings in a greater number of peaks. It is observed that, in all kinds of bearings, the increasing in the grooves depth causes an increase in the new pressure peaks magnitude generated, as well as an increase in the magnitude of the peaks that existed before the insertion of such grooves. Another fact to highlight is that the emergence of new peaks of pressure in the upper part of the bearing generates forces in the negative direction of z axis. These forces contribute in a negative form in the bearing load capacity, i.e. by increasing the number of grooves and their depth; there is a decrease in the bearing load capacity.

## 2.4 GENERAL COMMENTS

In all cases analyzed in this paper, the rotation of the shaft is always 6800rpm. At this speed, the fluid flow is in laminar regime, and therefore the consideration that the dissipated energy due to viscous effects is negligible ( $\xi = 0$ ) is perfectly acceptable, since this term would not bring any relevant information to the formulation.

The pressure used in all results presented in the study is the gauge pressure. Since the solution of Reynolds equation can give negative results of pressure, a relaxation process was used. The relaxation process used makes the negative part of the pressure field obtained to be null after each iteration. Thus, it is possible to obtain a solution closer to the reality of a bearing in operation, since, in practice, the bearing will always be submerged in oil, causing a positive pressure field.

The model was validated with both analytical results (model of short and long bearings) and with established numerical methods, such as the Finite Difference Method, and also with commercial software (PHOENICS). These validations can be seen in Machado (2011). Therefore, the initial objective of the paper, the parametric study performed on different type of bearings, could be achieved satisfactorily.

## 2.5 CONCLUSIONS

In this paper, the feasibility and benefits of using the finite volume method in the study and design of journal bearings with different geometries, smooth and grooved, under the condition of hydrodynamic lubrication, were evaluated. The model contemplated with satisfactory efficiency, the main objective of the paper as originally proposed, to evaluate the static behavior of different types of bearings.

In the results presented for the pressure distribution in the three different geometries of bearings with no grooves, it is important to evaluate the beneficial effect of increasing the number of lobes on the static behavior of the bearing. The increase in the magnitude of the pressure causes the load capacity of multilobular bearings being greater than for the case of cylindrical bearings.

After the grooves were introduced in the bearings, it might be noted that new peaks of pressure rose in their vicinity. It is also observed that the increasing in the depth of the grooves causes an increasing in the new peaks of pressure magnitude, as well as an increasing in the magnitude of the peaks that existed before the insertion of such grooves. In all bearings simulated here, the occurrence of new peaks of pressure in the upper part of the bearing contributes in a negative form in the bearing load capacity.

Overall, it is possible to conclude that the proposed numerical model is promising, and it can represent the physical phenomenon in a satisfactory way. Surely, it can bring contributions to the research related to hydrodynamic bearings and rotor dynamics.

## 3. ACKNOWLEDGEMENTS

The authors thank Schaeffler do Brasil for the financial and technical support for this research, as well as CNPq, CAPES and FAPESP for research funds.

## 4. REFERENCES

Arghir, M.; Alsayed, A.; Frêne, J.; *"A Triangle Based Finite Volume Method for the Integration of Lubrication's Incompressible Bulk Flow Equations"*; Journal of Tribology, Vol. 123, pp. 118-124, 2001.

Arghir, M.; Alsayed, A.; Nicolas, D.; "*The Finite Volume Solution of the Reynolds Equation of Lubrication with Film Discontinuities"*; International Journal of Mechanical Sciences, Vol. 44, pp. 2119-2132, 2002.

Castelli V.; Pirvics J.; *"Review of numerical methods in gas bearing film analysis"*; Journal of Lubrication Technology, n. 99(4), pp. 777–92, 1968.

Colin, W. C.; *"The method of Christopherson for Solving free Bondary Problems for Infinite Journal Bearings by Means of Finite Differences"*; Mathematics of Computation Corporation, Vol. 25, n. 115, 1971.

Dubois, G. B.; Ocvirk, F. W.; *"Analytical Derivation and Experimental Evaluation of Short Bearing Approximation for Full Journal Bearings"*; TN1157, NACA, 1953.

Hamrock, B. J.; Schmid, S. R.; Jacobson, B. O.; *"Fundamentals of Machine Elements"*, McGraw Hill, 2nd ed., New York, USA, pp. 325-539, 2005.

Kang, K.; Rhim, Y., Sung, K.; *"A study of the oil-lubricated Herringbone-Grooved journal bearing – Part 1: Numerical Analysis"*, Journal of Tribology, Vol. 118, pp. 906-911, 1996.

Kogure, K.; Fukui, S.; Mitsuya, Y.; Kaneko, R.; *"Design of Negative Pressure Slider for Magnetic Recording Discs"*; ASME Journal of Lubrication Technology, Vol. 105, p. 496-502, 1983.

Lund, J.; *"Review of the Concept of Dynamic Coefficients for Fluid Film Journal Bearings"*; ASME Journal of Tribology, Vol. 109, pp. 37- 41, 1987.

Machado, T. H.; Cavalca, K. L.; *"Evaluation of Dynamic Coefficients for Fluid Film Journal Bearings with Different Geometries",* In: 20th International Congress of Mechanical Engineering - COBEM 2009, Proceedings of the 20th International Congress of Mechanical Engineering, Gramado, Brazil, 2009.

Machado, T. H.; ***"****Avaliação de Mancais Hidrodinâmicos com Descontinuidades Geométricas"****;*** Campinas: Faculdade de Engenharia Mecânica, Universidade Estadual de Campinas, 2011. 122 p. Dissertação (Master Degree Dissertation).

Maliska, C. R.; *"Transferência de Calor e Mecânica dos Fluidos Computacional"*; Editora LTC, 2nd ed., Rio de Janeiro, Brasil, 2004.

Ocvirk, E W.; *"Short bearing approximation for full journal bearings"*; National Advisory Committee for Aeronautics, Cornell University, Technical Note 2808, 1952.

Patankar, S. V.; *"Numerical Heat Transfer and Fluid Flow"*, Hemisphere Publishing Corporation, 1st ed., Washington, 1980.

Petrov, N. P.; *"Friction in Machines and the Effect of Lubricant"*; Inzenernii Zhurnal, St. Petersburg, Vol. 1, pp. 71-140, Vol. 2, pp. 228-279, Vol. 3, pp. 377-436, Vol. 4, pp. 535-564, 1883.

Pinkus, O.; *"Analysis of Elliptical Bearings"*; Transactions of the ASME, Vol. 78, pp. 965-973, 1956.

Pinkus, O.; *"Solution of Reynolds Equation for Finite Journal Bearings"*; Transactions of ASME, Vol. 80, pp. 858-864, 1958.

Pinkus, O.; *"Analysis and Characteristics of Three-lobe Bearings"*; Journal of Basic Engineering, pp. 49-55, 1959.

Reynolds, O.; *"On the Theory of Lubrication and its Application to Mr. Beauchamp Tower's Experiments, including an Experimental Determination of the Viscosity of Olive Oil"*; Philosophical Transactions of Royal Society of London, Series A, Vol. 177, Part 1, pp.157-234, 1886.

Singhal, G. C.; *"Computation Methods for hydrodynamic problems (Reynold´s Equation)"*; Cumputer-Aided Design, Vol. 13, n. 3, pp. 151-154, 1981.

Sommerfeld, A.; *"Zur Hydrodynamischen Theorie der Schmiermittelreibung"*; Zs. Math. and Phys., Vol. 50, n. 1, pp. 97-155, 1904.

Tower, B.; *"Second report on friction experiments"*; *Proceedings of the Institution of Mechanical Engineers*, pp. 58-70, 1885.

## 5. RESPONSIBILITY NOTICE

The authors are the only responsible for the printed material included in this paper.